Resolving the octant of θ_{23} with T2K and NOνA

Sanjib Kumar Agarwalla,[a,b] **Suprabh Prakash,**[c] **S. Uma Sankar**[c]

[a]*Institute of Physics, Sachivalaya Marg, Sainik School Post, Bhubaneswar 751005, India*

[b]*Instituto de Física Corpuscular, CSIC-Universitat de València,*
Apartado de Correos 22085, E-46071 Valencia, Spain

[c]*Department of Physics, Indian Institute of Technology Bombay, Mumbai 400076, India*

E-mail: sanjib@iopb.res.in, suprabh@phy.iitb.ac.in, uma@phy.iitb.ac.in

ABSTRACT: Preliminary results of MINOS experiment indicate that θ_{23} is not maximal. Global fits to world neutrino data suggest two nearly degenerate solutions for θ_{23}: one in the lower octant (LO: $\theta_{23} < \pi/4$) and the other in the higher octant (HO: $\theta_{23} > \pi/4$). $\nu_\mu \to \nu_e$ oscillations in superbeam experiments are sensitive to the octant and are capable of resolving this degeneracy. We study the prospects of this resolution by the current T2K and upcoming NOνA experiments. Because of the hierarchy-$\delta_{\rm CP}$ degeneracy and the octant-$\delta_{\rm CP}$ degeneracy, the impact of hierarchy on octant resolution has to be taken into account. As in the case of hierarchy determination, there exist favorable (unfavorable) values of $\delta_{\rm CP}$ for which octant resolution is easy (challenging). However, for octant resolution the unfavorable $\delta_{\rm CP}$ values of the neutrino data are favorable for the anti-neutrino data and vice-versa. This is in contrast to the case of hierarchy determination. In this paper, we compute the combined sensitivity of T2K and NOνA to resolve the octant ambiguity. If LO is the true octant, then NOνA can rule out HO at 2σ C.L., irrespective of the hierarchy and $\delta_{\rm CP}$. Addition of T2K data improves the octant sensitivity. If HO and normal hierarchy are the true choices, then the combined data from NOνA and T2K with its designed five years run in neutrino mode, is incapable of a 2σ resolution of the octant for all $\delta_{\rm CP}$. A 2σ resolution of the octant, for all combinations of neutrino parameters, becomes possible if T2K has balanced neutrino and anti-neutrino runs of 2.5 years each.

Contents

1 Introduction and Motivation

Our understanding of the smallest lepton mixing angle θ_{13} has improved quite dramatically in last one year or so and finally it has been confirmed to be non-zero with unprecedented confidence by the reactor experiments Daya Bay [1] and RENO [2]. They have found a reasonably large 1-3 mixing

$$\sin^2 2\theta_{13}|_{\textbf{DayaBay}} = 0.089 \pm 0.010\,(\text{stat}) \pm 0.005\,(\text{syst})\;[3], \text{ and}$$

$$\sin^2 2\theta_{13}\big|_{\textbf{RENO}} = 0.113 \pm 0.013\,(\text{stat}) \pm 0.019\,(\text{syst})\;[4],$$

in agreement with the measurements performed earlier by T2K [5, 6], MINOS [7, 8], and Double Chooz [9, 10] experiments. Combined analyses of all the neutrino oscillation data available [11–13] imply a non-zero value of θ_{13} at more than 10σ and predict a best-fit value of $\sin^2\theta_{13} \simeq 0.023$ with a relative 1σ precision of 10%. These recent high precision measurements of θ_{13} have taken us one step further in validating the standard three flavor oscillation picture of neutrinos on a strong footing [14]. Also, a moderately large value of θ_{13} has provided a *'golden'* opportunity to directly determine the neutrino mass hierarchy[1] (NMH) using the Earth matter effects, and to unravel the evidence of leptonic CP violation (LCPV)[2] in accelerator based long baseline neutrino oscillation experiments [15].

---

[1]Two possibilities are there: it can be either normal (NH) if $\Delta_{31} \equiv m_3^2 - m_1^2 > 0$, or inverted (IH) if $\Delta_{31} < 0$.

[2]If the Dirac CP phase, $\delta_{\rm CP}$ differs from 0 or π.

Another recent and crucial development is the indication of non-maximal θ_{23} by the MINOS accelerator experiment [8]. However, the atmospheric neutrino data, dominated by Super-Kamiokande, still prefers the maximal value of θ_{23} [16]. All the three global fits of world neutrino data [11–13] also point to the deviation from maximal mixing for θ_{23} *i.e.* $|0.5 - \sin^2\theta_{23}| \neq 0$.

Both these new measurements, non-zero value of θ_{13} and non-maximal θ_{23}, will provide crucial inputs to the theories of neutrino masses and mixings [17–20]. A number of innovative ideas, such as $\mu \leftrightarrow \tau$ symmetry [21–29], A_4 flavor symmetry [30–34], and quark-lepton complementarity [35–38] have been invoked to explain the observed pattern of one small and two large mixing angles in the neutrino sector. Measurements of the precise values of θ_{13} and θ_{23} will reveal the pattern of deviations from these symmetries and will lead to a better understanding of neutrino masses and mixings. In particular, the resolution of θ_{23} octant will severely constrain the patterns of symmetry breaking.

In ν_μ survival probability, the dominant term is mainly sensitive to $\sin^2 2\theta_{23}$. Now, if $\sin^2 2\theta_{23}$ differs from 1 as indicated by the recent neutrino data, then we get two solutions for θ_{23}: one $< \pi/4$, termed as lower octant (LO) and the other $> \pi/4$, termed as higher octant (HO). In other words, if the quantity $(0.5 - \sin^2\theta_{23})$ is positive (negative) then θ_{23} belongs to LO (HO). This is known as the octant degeneracy of θ_{23} [39] which is a part of the overall eight-fold degeneracy [40, 41], where the other two degeneracies are $(\theta_{13}, \delta_{\mathrm{CP}})$ intrinsic degeneracy [42] and the (hierarchy, δ_{CP}) degeneracy [43].

The octant ambiguity of θ_{23} is considered to be the most difficult one to deal with among the eight-fold parameter degeneracies. In the past when we had only an upper bound on θ_{13}, a possible way of resolving this degeneracy by combining future reactor data with accelerator ν_μ disappearance and ν_e appearance measurements was suggested in [44, 45]. Adding the information from the 'silver' channel ($\nu_e \to \nu_\tau$) to the 'golden' channel ($\nu_e \to \nu_\mu$) in the proposed neutrino factory setup is demonstrated to be one of the elegant ways to tackle this degeneracy [46, 47]. The possibility of determining the deviation of θ_{23} from maximal mixing and consequently the correct octant of θ_{23} in very long baseline neutrino oscillation experiments and as well as in future atmospheric neutrino experiments has been discussed in [48–56]. One clear message that has been conveyed by all these novel works is that one can achieve a very good sensitivity to the quantity $|0.5 - \sin^2\theta_{23}|$ from the conventional beam experiments (MINOS, ICARUS and OPERA), the current generation superbeam experiments (presently running T2K and upcoming NOνA), and also from the current (Super-Kamiokande) and future atmospheric data (India-based Neutrino Observatory). But, determining the sign of $|0.5 - \sin^2\theta_{23}|$ is deemed to be a very difficult job to pursue and it demands a large value of θ_{13}.

Now, in the light of recently discovered moderately large value of θ_{13}, it would be quite interesting to study whether the expected appearance data from the ongoing T2K experiment [6, 57] in Japan and the upcoming NOνA experiment [58, 59] in the United States can resolve the octant ambiguity of θ_{23} or not? In this paper, we address this issue.

The structure of the paper is as follows. We start in section 2 by revisiting our present understanding of the 2-3 mixing angle. Section 3 describes in detail the physics issues related to the octant of θ_{23}. We show the event rates for T2K and NOνA in section 4. At

the end of this section, we also describe the simulation method followed. We present our results in section 5. Finally, in section 6, we summarize and draw our conclusions. Expected events rates in T2K and NOνA (both for neutrino and anti-neutrino) as a function of $\delta_{\rm CP}$ can be found in Appendix A. Allowed regions in the $\sin^2 \theta_{23}({\rm test})$ - $\delta_{\rm CP}({\rm test})$ plane for the true value of $\delta_{\rm CP} = 0$ and all the four combinations of true hierarchy and true octant are shown in Appendix B.

2   Present Understanding of the 2-3 mixing angle

Our present knowledge of θ_{23} comes from two sources: a) atmospheric neutrinos and b) accelerator neutrinos. In both cases, the muon neutrino disappearance is parametrized in the form of two-flavor survival probability

$$ {\rm P}_{\mu\mu} = 1 - \sin^2 2\theta_{\rm eff} \sin^2 \left(\frac{\Delta m^2_{\rm eff} L}{4E} \right). \tag{2.1} $$

Analysis of the data gives reasonably precise values for the effective two-flavor parameters. Relating these to the three flavor parameters depends on the experimental set up. In the case of atmospheric neutrinos, the path lengths involved vary from 20 km to 13000 km and the energies vary from 200 MeV to a few GeV. This represents a very wide range in L/E. The approximations valid for some values of L/E are not valid for others. Therefore, for atmospheric neutrinos, it is not possible to obtain a direct relation between the effective two-flavor parameters and the three-flavor parameters. However, for accelerator neutrinos, L and E are chosen so that $\Delta_{31} L/E \sim \pi/2$. Hence, $\Delta_{21} L/E \ll 1$ $(\Delta_{21} = m_2^2 - m_1^2)$ and can be treated as a small perturbation. In this approximation, it was shown that [60–62]

$$ \Delta m^2_{\rm eff} = \Delta_{31} - \left(\cos^2 \theta_{12} - \cos \delta_{\rm CP} \sin \theta_{13} \sin 2\theta_{12} \tan \theta_{23} \right) \Delta_{21}, \tag{2.2} $$

$$ \sin^2 2\theta_{\rm eff} = 4 \cos^2 \theta_{13} \sin^2 \theta_{23} \left(1 - \cos^2 \theta_{13} \sin^2 \theta_{23} \right). \tag{2.3} $$

The mixing angles and phases are defined according to the Particle Data Group convention [63]. The atmospheric neutrino data, dominated by Super-Kamiokande, still prefers the maximal value of $\sin^2 2\theta_{\rm eff} = 1\,(\geq 0.94\,(90\%\,{\rm C.L.}))$ [16]. But the preliminary results from the MINOS accelerator experiment favor a non-maximal value of $\sin^2 2\theta_{\rm eff} = 0.94^{+0.04}_{-0.05}$ [8].

Reference	Forero et.al. [11]	Fogli et.al. [12]	Gonzalez-Garcia et.al. [13]
$\sin^2 \theta_{23}$ (NH)	$0.427^{+0.034}_{-0.027} \oplus 0.613^{+0.022}_{-0.040}$	$0.386^{+0.024}_{-0.021}$	$0.41^{+0.037}_{-0.025} \oplus 0.59^{+0.021}_{-0.022}$
3σ range	$0.36 \to 0.68$	$0.331 \to 0.637$	$0.34 \to 0.67$
$\sin^2 \theta_{23}$ (IH)	$0.600^{+0.026}_{-0.031}$	$0.392^{+0.039}_{-0.022}$	
3σ range	$0.37 \to 0.67$	$0.335 \to 0.663$	

Table 1: 1σ bounds on $\sin^2 \theta_{23}$ from the global fits performed in References [11], [12], and [13]. NH and IH stand for normal and inverted hierarchies. The numbers cited from Ref. [13] are those obtained by keeping the reactor fluxes free in the fit and also including the short baseline reactor data with $L \lesssim 100$ m, with the mass hierarchy marginalized.

Global fits, using three-flavor oscillations, give information directly on θ_{23} rather than θ_{eff}. The best-fit values and ranges of θ_{23} from the three recent global fits [11], [12], and [13] are listed in Table 1. A common feature that has emerged from all the three global fits of the world neutrino data is that we now have indication for non-maximal θ_{23}. Thus, we have the two degenerate solutions: either θ_{23} belongs to the LO ($\sin^2 \theta_{23} \approx 0.4$) or it lies in the HO ($\sin^2 \theta_{23} \approx 0.6$). This degeneracy, in principle, can be broken with the help of $\nu_\mu \leftrightarrow \nu_e$ oscillation data. The preferred value would depend on the choice of the neutrino mass hierarchy. However, as can be seen from Table 1, the fits of reference [11] do not agree on which value should be preferred, even when the mass hierarchy is fixed to be NH. In [12], LO is preferred over HO for both NH and IH. Reference [13] marginalizes over the mass hierarchy, so the degeneracy remains. The global best-fits in references [11, 13] do not observe any sensitivity to the octant of θ_{23} unless they add the atmospheric neutrino data. But, in [12], they do find a preference for LO even without adding the atmospheric data. In this paper, we take the best-fit value of $\sin^2 \theta_{23}$ in the lower octant (LO) to be 0.41 while that in the higher octant (HO) to be 0.59 [13].

3   Physics of the octant of θ_{23}

In a long baseline experiment, ν_μ charged current (CC) events are the most copious. These experiments can measure $\nu_\mu \to \nu_\mu$ survival probability, $\mathrm{P}_{\mu\mu}$, as a function of energy. The reconstruction of the minimum of $\mathrm{P}_{\mu\mu}$ leads to precise values for $|\Delta m^2_{\mathrm{eff}}|$ and $\sin^2 2\theta_{\mathrm{eff}}$ [8, 60–62]. Therefore, we get two degenerate best fit values for $\sin^2 \theta_{23}$, one in LO and the other in HO, with small allowed regions around them. The $\mathrm{P}_{\mu\mu}$ expression has subleading terms which are sensitive to octant [64]. But, these are suppressed by the small parameter $\alpha = \Delta_{21}/\Delta_{31}$ and their biggest impact occurs for energies where $\mathrm{P}_{\mu\mu}$ is very small. So, the overall octant sensitivity of $\mathrm{P}_{\mu\mu}$ is negligible. However, $\mathrm{P}_{\mu\mu}$ gives a precise measurement of $\sin^2 2\theta_{\mathrm{eff}}$ which in turn gives precise allowed regions for $\sin^2 \theta_{23}$ in the two octants.

In the presence of matter, the $\nu_\mu \to \nu_e$ oscillation probability, expanded perturbatively in α, can be written as [64–66]

$$P_{\mu e} = \beta_1 \sin^2 \theta_{23} + \beta_2 \cos(\hat{\Delta} + \delta_{\mathrm{CP}}) + \beta_3 \cos^2 \theta_{23}. \tag{3.1}$$

In the above equation, $P_{\mu e}$ is written in a way to highlight the octant and δ_{CP} dependent terms. Here

$$\beta_1 = \sin^2 2\theta_{13} \frac{\sin^2 \hat{\Delta}(1-\hat{A})}{(1-\hat{A})^2},$$

$$\beta_2 = \alpha \cos \theta_{13} \sin 2\theta_{12} \sin 2\theta_{13} \sin 2\theta_{23} \frac{\sin \hat{\Delta}\hat{A}}{\hat{A}} \frac{\sin \hat{\Delta}(1-\hat{A})}{1-\hat{A}},$$

$$\beta_3 = \alpha^2 \sin^2 2\theta_{12} \cos^2 \theta_{13} \frac{\sin^2 \hat{\Delta}\hat{A}}{\hat{A}^2}, \tag{3.2}$$

with $\hat{\Delta} = \Delta_{31}L/4E$, $\hat{A} = A/\Delta_{31}$. A is the Wolfenstein matter term [67] and is given by $A(\mathrm{eV}^2) = 0.76 \times 10^{-4}\rho$ (g/cc)E(GeV). ρ is the density of matter in the Earth. For NOνA and T2K, this is set equal to the density in the crust of 2.8 g/cc.

For normal hierarchy (NH), Δ_{31} is positive and for inverted hierarchy (IH), it is negative. The matter term A is positive for neutrinos and is negative for anti-neutrinos. Hence, in neutrino oscillation probability, $\hat{A}$ is positive for NH and is negative for IH; vice-verse for anti-neutrinos. Moreover, sign of δ_{CP} is reversed for anti-neutrinos. The left(right) panel of figure 1 shows $P_{\mu e}$ .vs. E_ν ($P_{\bar{\mu}\bar{e}}$ .vs. $E_{\bar{\nu}}$) for all possible values of δ_{CP} and for the two values of $\sin^2\theta_{23}$, assuming NH to be the true hierarchy. These plots are for the experiment NOνA .
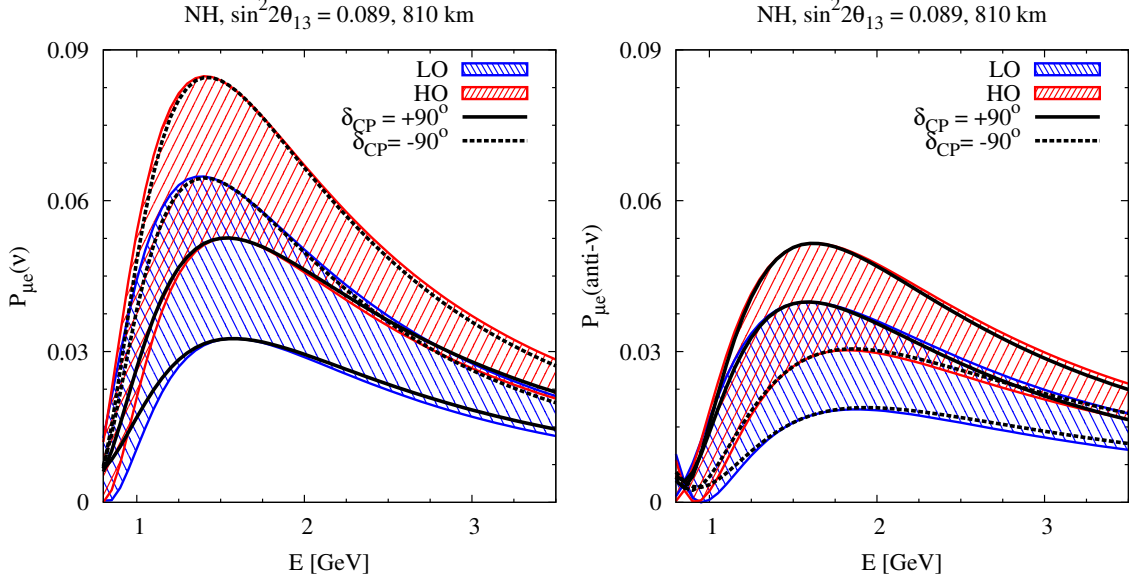
Figure 1: $P_{\mu e}$ as a function of neutrino energy. The left panel (right panel) is for ν ($\bar{\nu}$). Here, the bands correspond to different values of δ_{CP} from $-\pi$ to π. These plots are for NOνA (L=810 km), $\sin^2 2\theta_{13} = 0.089$ and NH. For LO(HO), $\sin^2\theta_{23} = 0.41(0.59)$.

As can be seen from these figures, there is an overlap between the two octant bands for some values of δ_{CP}. This overlap spoils the octant determination sensitivity of the experiment. Those combinations of octant and δ_{CP} which lie farthest from the overlap will be the favorable combinations while the overlapping combinations will be the unfavorable ones. For favorable combinations, octant degeneracy can easily be resolved while it is difficult for unfavorable ones. A comparison of left and right panels leads to a very interesting observation. For the ν case, the favorable combinations are (HO, $\delta_{CP} \sim -90°$) and (LO, $\delta_{CP} \sim 90°$). However, for the $\bar{\nu}$ case, the the favorable δ_{CP} values for HO are $\sim 90°$ while those for LO are $\sim -90°$. Similar arguments hold for IH also. This is in contrast to the hierarchy-δ_{CP} degeneracy, where for a given hierarchy, the favorable δ_{CP} region is the same for both ν and $\bar{\nu}$. Thus, we are led to the conclusion that a balanced neutrino and anti-neutrino data is imperative for resolving the octant for all values of δ_{CP}.

Let us do a small, quantitative analysis of the octant-δ_{CP} degeneracy of P$_{\mu e}$. For simplicity, here we keep the hierarchy fixed. Increase in θ_{23} increases $P_{\mu e}$. While a change in δ_{CP} can increase or decrease $P_{\mu e}$. For different δ_{CP}^{LO} and δ_{CP}^{HO}, $P_{\mu e}(LO, \delta_{CP}^{LO})$ may be very

close to $P_{\mu e}(\text{HO}, \delta_{\text{CP}}^{\text{HO}})$. For the degenerate case, $P_{\mu e}(\text{LO}, \delta_{\text{CP}}^{\text{LO}}) = P_{\mu e}(\text{HO}, \delta_{\text{CP}}^{\text{HO}})$, leading to

$$\cos(\hat{\Delta} + \delta_{\text{CP}}^{\text{LO}}) - \cos(\hat{\Delta} + \delta_{\text{CP}}^{\text{HO}}) = \frac{\beta_1 - \beta_3}{\beta_2}(\sin^2\theta_{23}^{\text{HO}} - \sin^2\theta_{23}^{\text{LO}}). \tag{3.3}$$

For the NOνA baseline L = 810 km and energy of peak flux E = 2 GeV, we get for NH and ν

$$\cos(\hat{\Delta} + \delta_{\text{CP}}^{\text{LO}}) - \cos(\hat{\Delta} + \delta_{\text{CP}}^{\text{HO}}) = 1.7. \tag{3.4}$$

The above equation will have solutions only if

$$0.7 \leq \cos(\hat{\Delta} + \delta_{\text{CP}}^{\text{LO}}) \leq 1.0,$$
$$-1.0 \leq \cos(\hat{\Delta} + \delta_{\text{CP}}^{\text{HO}}) \leq -0.7. \tag{3.5}$$

From this, we get their ranges to be:

$$-116° \leq \delta_{\text{CP}}^{\text{LO}} \leq -26°,$$
$$64° \leq \delta_{\text{CP}}^{\text{HO}} \leq 161°. \tag{3.6}$$

Thus, we find that for NH and ν of energy 2 GeV, $P_{\mu e}(\text{LO}, -116° \leq \delta_{\text{CP}} \leq -26°)$ is degenerate with $P_{\mu e}(\text{HO}, 64° \leq \delta_{\text{CP}} \leq 161°)$. A similar analysis can be done for T2K baseline of L = 295 km and energy of peak flux E = 0.8 GeV. The overlap regions in the δ_{CP} range are essentially the same as above because the values of $\hat{\Delta}$ and those of $(\beta_1 - \beta_3)/\beta_2$ are nearly the same for the two experiments. This is to be contrasted with the hierarchy discrimination, where the overlap range for NOνA is very different from that of T2K because of widely different matter effects [68, 69].

In figure 2, we show the values of δ_{CP}, which lie in the overlapping region, as a function of energy, for the combinations LO-NH and HO-NH. For NOνA experiment, most of the signal events come from the range 1.5 - 2.5 GeV. Hence, we consider only this energy range in the figure. The blue-dotted (red-crossed) shaded region shows those values of δ_{CP}, for which there is an overlap between $P_{\mu e}^{\text{LO}}$ and $P_{\mu e}^{\text{HO}}$, for ν ($\bar{\nu}$) data. These plots show the degenerate octant-δ_{CP} values in the relevant energy range and help explain the δ_{CP} dependence seen in octant sensitivity.

The values of δ_{CP} which lie farthest from any of the overlap regions will be the most favored ones. Those δ_{CP} values which lie in one of the overlap region (i.e. either in ν or $\bar{\nu}$) but are far from the other overlap region will also be favored (though to a lesser extent than the previous values) if balanced ν and $\bar{\nu}$ runs are taken. The regions of δ_{CP} which are common or very close to both overlap regions will be the most unfavored ones. We find that $\delta_{\text{CP}} \sim 0$ is the most unfavorable for LO-NH and HO-IH whereas $\delta_{\text{CP}} \sim 180°$ is the most unfavorable for HO-NH and LO-IH. This pattern is observed in the results in subsection 5.1.

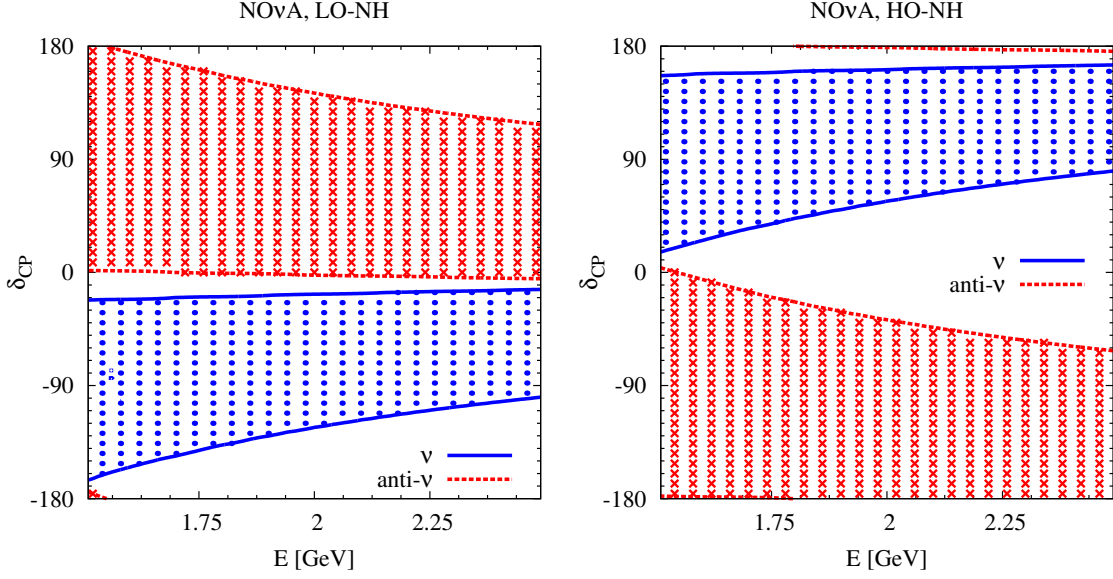**Figure 2**: Plots showing octant-δ_{CP} degeneracy in $P_{\mu e}$ as a function of neutrino energy. The left (right) panel is for LO (HO). The blue-dotted (red-crossed) regions are for ν ($\bar{\nu}$). For a given $E_\nu(E_{\bar{\nu}})$, $P_{\mu e}[$ LO, *vertical blue-dotted (red-crossed) δ_{CP} region in the left panel*] values are degenerate with $P_{\mu e}[$ HO, *vertical blue-dotted (red-crossed) δ_{CP} region in the right panel*] values. The exact degenerate octant-δ_{CP} values can be found out using equation 3.4. As an example, for E_ν of 2 GeV, $P_{\mu e}$ (LO, $\delta_{CP} = -90°$) is degenerate with $P_{\mu e}$(HO, $\delta_{CP} \approx 66°$). These plots are for NOνA (L=810 km), $\sin^2 2\theta_{13} = 0.089$ and NH. For LO(HO), $\sin^2 \theta_{23} = 0.41(0.59)$.

4 Event Rates for T2K and NOνA

In this paper, we simulate the data for the two *off-axis* superbeam experiments: T2K and NOνA using GLoBES [70, 71]. In the T2K experiment, a ν_μ beam from J-PARC is directed towards Super-Kamiokande detector, 295 km away. The flux peaks sharply at 0.8 GeV, close to the first oscillation maximum in $P(\nu_\mu \to \nu_e)$. The experiment is scheduled to run for 5 years in the neutrino mode only. The details of T2K experiment are given in [57]. The information regarding signal efficiencies and backgrounds are taken from [72, 73]. NOνA is a 14 kT totally active scintillator detector located at Ash River; a distance of 810 km from Fermilab. The flux peaks at 2 GeV, again close to the first oscillation maximum in $P(\nu_\mu \to \nu_e)$. This experiment is scheduled to have three years run in neutrino mode first and then later, three years run in anti-neutrino mode as well. The details of the experiment are given in [74]. In light of the recent measurement of large θ_{13}, NOνA has reoptimized their signal and background acceptances. In our calculations, we use these reoptimized values, the details of which are given in [59, 75].

In our simulations, we have used the following input values for neutrino oscillation

parameters [8, 13].

$$|\Delta m^2_{\text{eff}}| = 2.4 \times 10^{-3}\,\text{eV}^2$$
$$\Delta_{21} = 7.5 \times 10^{-5}\,\text{eV}^2, \qquad \sin^2\theta_{12} = 0.3$$
$$\sin^2 2\theta_{13} = 0.089$$

The value of Δ_{31} is calculated separately for NH and for IH using equation 2.2 where Δm^2_{eff} is taken to be +ve for NH and -ve for IH. The uncertainties in the above parameters are taken to be $\sigma(|\Delta m^2_{\text{eff}}|) = 4\%$ [8] and $\sigma(\sin^2 2\theta_{13}) = 5\%$ [76]. The solar parameters (Δ_{21} and $\sin^2\theta_{12}$) and the Earth matter density in the calculation of matter term are held fixed throughout the calculation.
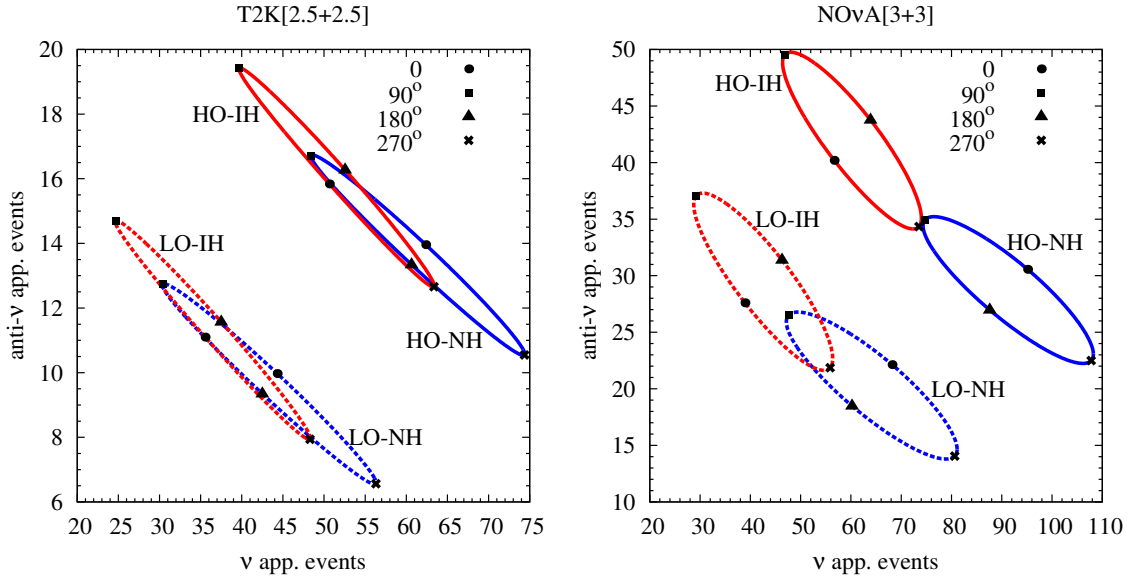
Figure 3: ν and $\bar{\nu}$ appearance events for all possible combinations of hierarchy, octant and δ_{CP}. The left (right) panel is for T2K (NOνA). Here $\sin^2 2\theta_{13} = 0.089$. For LO(HO), $\sin^2\theta_{23} = 0.41(0.59)$. Note that for T2K, equal ν and $\bar{\nu}$ runs of 2.5 years each has been assumed.

In figure 3[3], we plot ν events .vs. $\bar{\nu}$ events for various octant-hierarchy combinations. In each case, with varying values of δ_{CP}, the plot becomes an ellipse. The left panel shows these ellipses for T2K whereas the right panel shows the same for NOνA . *Here, we assumed that T2K will have equal ν and $\bar{\nu}$ runs of 2.5 years each.* In the right panel, we see that the ellipses for the two hierarchies overlap whereas the ellipses of LO are well separated from those of HO. Hence, we can expect that NOνA will have better octant discrimination capability than hierarchy discrimination. This situation is even more dramatic in the left panel where there is large overlap between the two hierarchies but clear separation between the octants. Thus, it is very likely that $\bar{\nu}$ data from T2K may play an important role in the determination of octant.

---

[3]The variation of ν and $\bar{\nu}$ appearance events with δ_{CP} is shown in appendix A for both T2K and NOνA .

We illustrate the octant determination capability of NOνA by considering some special points in the right panel. The features that we emphasize here can also be discerned from figure 2.

- <u>LO-NH, $\delta_{\rm CP} = 0°$</u>: The coordinates of this point in the ν-$\bar{\nu}$ event plane are (70,23). No point on the HO-NH ellipse has these coordinates but there exist a number of points with coordinates close to these. Therefore, the wrong octant is difficult to rule out for this point.

- <u>LO-NH, $\delta_{\rm CP} = 90°$</u>: The coordinates of this point in the ν-$\bar{\nu}$ event plane are (50,26). The ν events are much lower than those of all points on the HO-NH ellipse but there is degeneracy in the $\bar{\nu}$ events. Hence, ruling out the wrong octant should be possible for this point.

- <u>LO-NH, $\delta_{\rm CP} = 180°$</u>: The coordinates of this point in the ν-$\bar{\nu}$ event plane are (62,18). Both ν and $\bar{\nu}$ events are much lower than the corresponding events of any point on the HO-NH ellipse. Thus, ruling out the wrong octant will be the easiest for this point.

- <u>LO-NH, $\delta_{\rm CP} = -90°$</u>: An argument similar to the case $\delta_{\rm CP} = 90°$ can be made, except that the ν events have degeneracy between octants, but the $\bar{\nu}$ events for this point are much below those of any point on the HO-NH ellipse.

Similar arguments can be made for other octant-hierarchy combinations with the exception that the most favorable and most unfavorable $\delta_{\rm CP}$ values will differ.

We see that for the given choice of best-fit values of $\sin^2 \theta_{23}$, NOνA has very good sensitivity to octant resolution due to balanced ν and $\bar{\nu}$ runs. Because the favorable and unfavorable values of $\delta_{\rm CP}$ (pertaining to octant resolution) are different for ν and $\bar{\nu}$, no $\delta_{\rm CP}$ value is absolutely unfavorable if balanced ν and $\bar{\nu}$ runs are taken. Therefore, a single experiment on its own, can have very good sensitivity as illustrated in figure 3. This is in stark contrast to the case of hierarchy, where we saw that having data from two experiments with widely different baseline is a necessity because the favorable and unfavorable combinations turned out to be the same for ν and $\bar{\nu}$.

Before discussing our results, we briefly describe the numerical procedure adopted. We calculate $\Delta\chi^2$ using the default definition in GLoBES which is Poissonian. We minimize this $\Delta\chi^2$ to compute the octant resolution capability. For a given octant-hierarchy combination and a true value of $\delta_{\rm CP}$, we compute the events spectra and label it *data*. Then we compute the theoretical events spectra where the octant is chosen to be the wrong one and the neutrino parameters are randomly chosen within their allowed 3σ ranges. We then calculate the $\Delta\chi^2$ between the data and the theoretical spectra. This calculation uses the $\Delta\chi^2$ defined in GLoBES, which is valid for a Poissonian distribution. We add a $\Delta\chi^2$ coming from gaussian priors on $|\Delta m^2_{\rm eff}|$ and on $\sin^2 2\theta_{13}$. The systematic uncertainties are included using the method of pulls. If the $\Delta\chi^2_{\rm min} \geq 4$, then we can say that the wrong octant is ruled out at 2σ for the given combination and the given true value of $\delta_{\rm CP}$. This calculation is repeated for all true values of $\delta_{\rm CP}$ and for all combinations. If the $\Delta\chi^2_{\rm min} \geq 4$

in each case then the wrong octant can be ruled out independently of true δ_{CP}, hierarchy and octant.

5 Results

In this section, through various plots, we show the sensitivity of T2K and NOνA to the octant of θ_{23}.

5.1 Allowed regions in test $\sin^2\theta_{23}$ - true δ_{CP} plane

In figures 4-7, we have plotted the values of test $\sin^2\theta_{23}$ allowed by T2K and NOνA data as a function of true δ_{CP} for each of the four combinations of octant and hierarchy. In our calculations, we do not assume a prior knowledge of hierarchy and hence consider both the possibilities for test hierarchy. Octant can be determined only if the wrong octant values are ruled out for both possibilities.

In this analysis, we have included the data from both the disappearance channel $P_{\mu\mu}$ and the appearance channel $P_{\mu e}$. We varied $\sin^2\theta_{23}$ within its 3σ range: [0.34, 0.67] allowed by the current global fits. Here, we are constraining $\sin^2\theta_{23}$ only and are marginalizing over δ_{CP} and hence take the 2σ limit relevant for 1 d.o.f. The contours in these figures are defined by $\Delta\chi^2 \leq 4$. *The disappearance channel gives a precise measurement of* $\sin^2 2\theta_{eff}$ *which leads to two narrow, δ_{CP}-independent, allowed $\sin^2\theta_{23}$ bands, one in each octant. The appearance channel, because of its large octant sensitivity, discriminates against the wrong octant band.* If the statistics are large enough, the wrong octant can be ruled out.
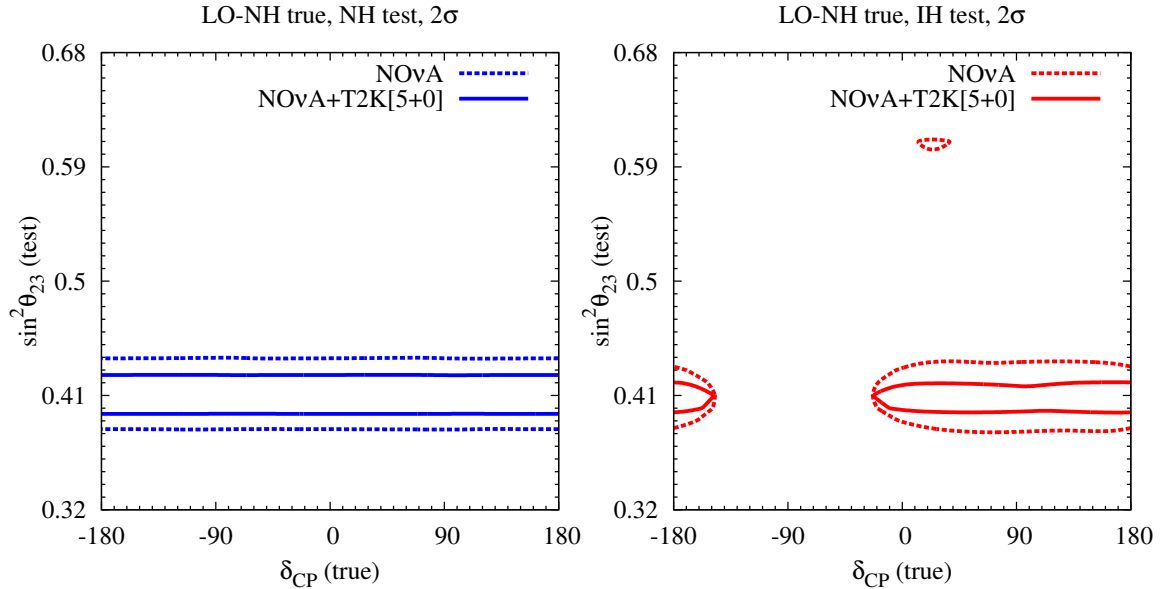

Figure 4: Allowed values of test $\sin^2\theta_{23}$ at 2σ (1 d.o.f.) C.L. as a function of true δ_{CP}. LO-NH is assumed to be the true octant-hierarchy combination. The left (right) panel corresponds to NH (IH) being the test hierarchy.

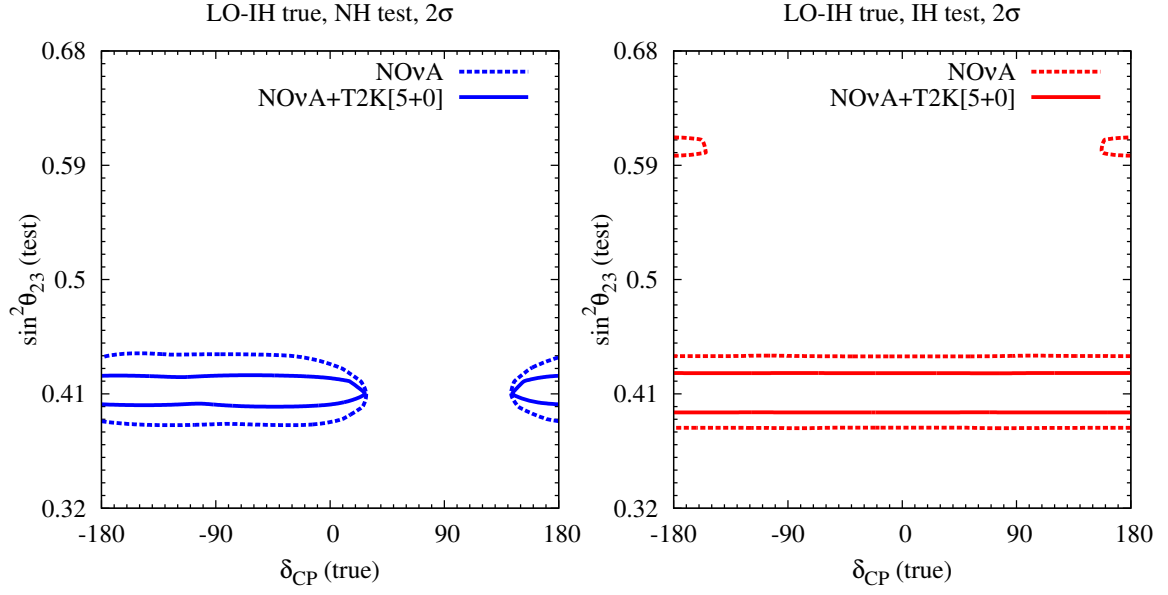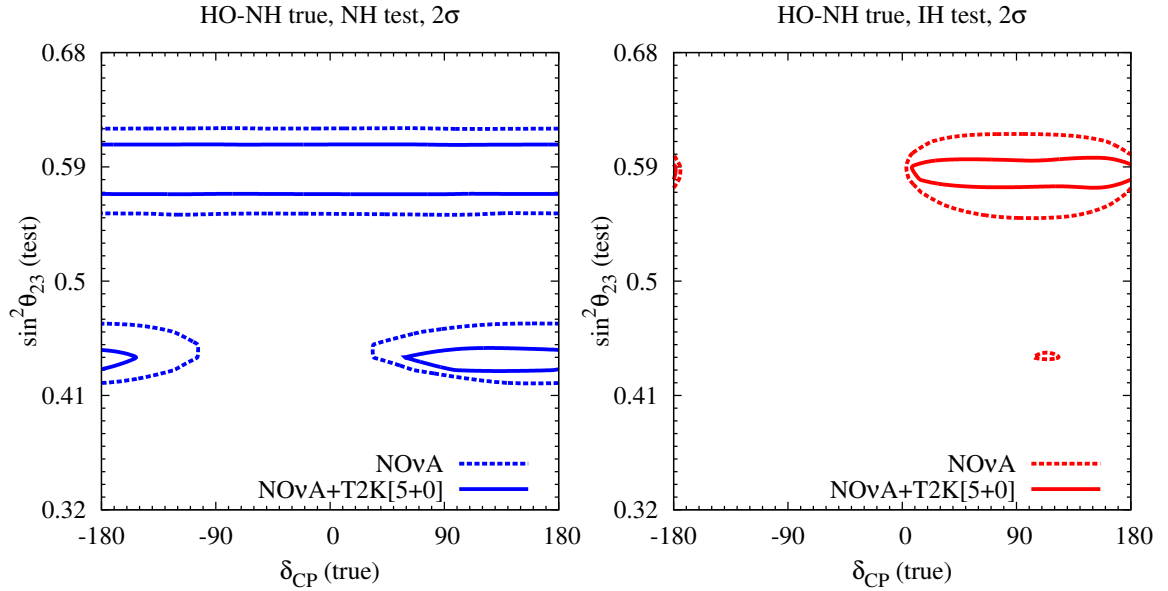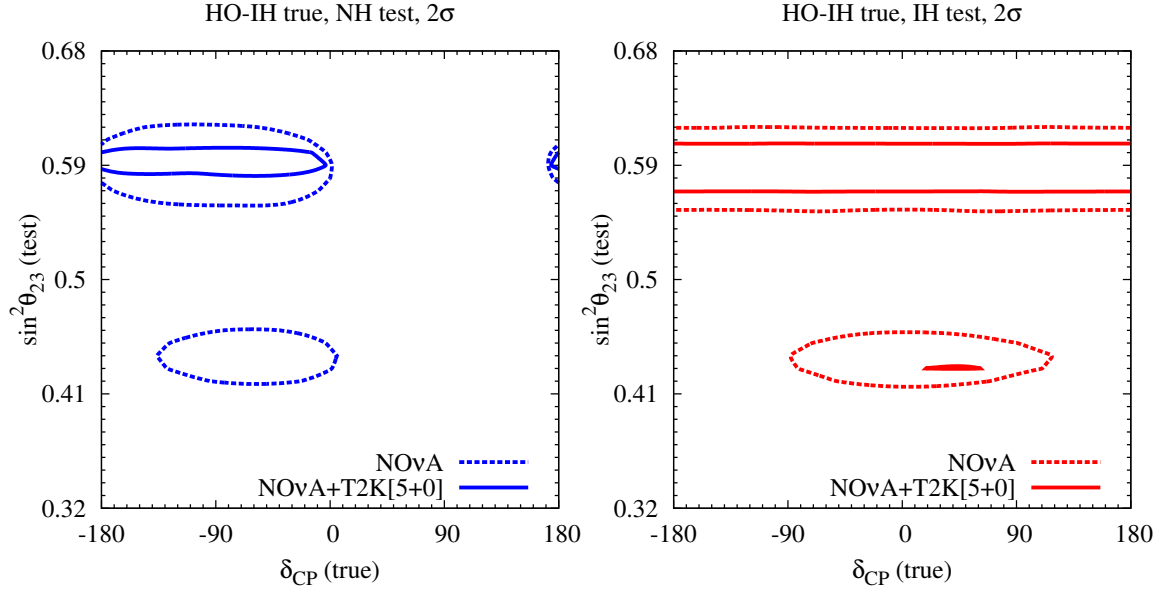**Figure 5**: Allowed values of test $\sin^2\theta_{23}$ at 2σ (1 d.o.f.) C.L. as a function of true δ_{CP}. LO-IH is assumed to be the true octant-hierarchy combination. The left (right) panel corresponds to NH (IH) being the test hierarchy.
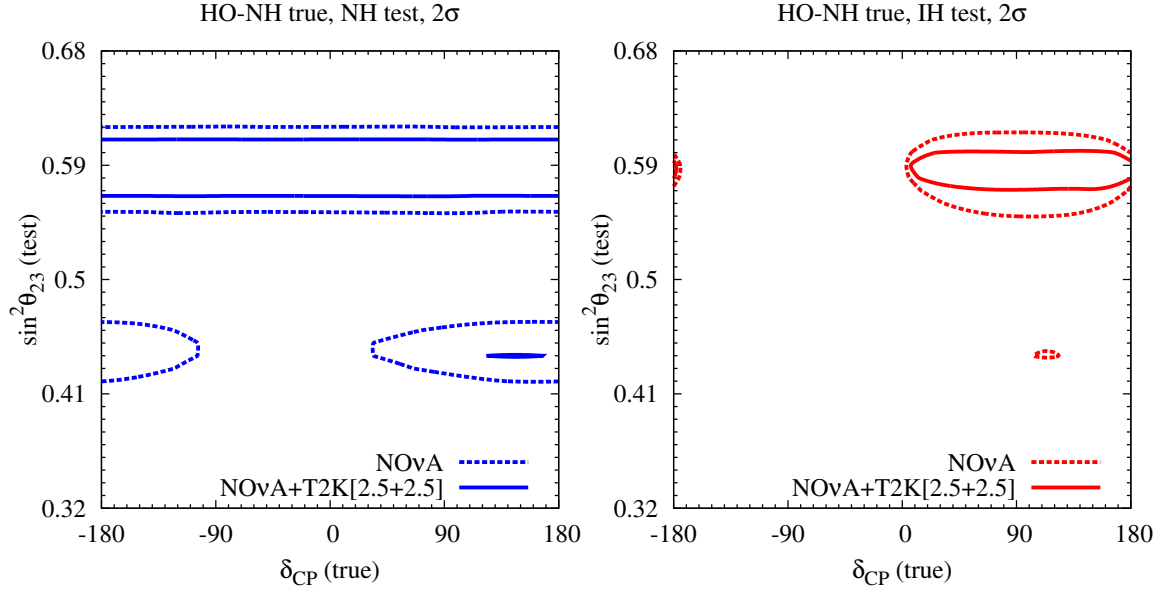

Figure 6: Allowed values of test $\sin^2\theta_{23}$ at 2σ (1 d.o.f.) C.L. as a function of true δ_{CP}. HO-NH is assumed to be the true octant-hierarchy combination. The left (right) panel corresponds to NH (IH) being the test hierarchy.

Figure 7: Allowed values of test $\sin^2\theta_{23}$ at 2σ (1 d.o.f.) C.L. as a function of true δ_{CP}. HO-IH is assumed to be the true octant-hierarchy combination. The left (right) panel corresponds to NH (IH) being the test hierarchy.

Figure 8: Allowed values of test $\sin^2\theta_{23}$ at 2σ (1 d.o.f.) C.L. as a function of true δ_{CP}. HO-NH is assumed to be the true octant-hierarchy combination. The left (right) panel corresponds to NH (IH) being the test hierarchy. Note that for T2K, equal ν and $\bar{\nu}$ runs of 2.5 years each has been assumed.

From figures 4 and 5, we note that the combined data of T2K and NOνA can rule out

HO if LO is the true octant. This holds for both NH and IH. However, if HO is the true octant, then LO can not be ruled out for a reasonably large fraction of true δ_{CP}.

As argued in section 3, the favorable and unfavorable regions are very different for neutrinos and anti-neutrinos. Hence, we explored if an improvement in the octant determination can be achieved if T2K has equal neutrino and anti-neutrino runs of 2.5 years each[4]. As expected, in the two cases of LO-NH and LO-IH, a $(2.5\nu + 2.5\bar{\nu})$ runs in T2K is also effective in ruling out the wrong octant at 2σ. Hence, we have not displayed the corresponding figures. But, for the two cases HO-NH and HO-IH, the balanced ν and $\bar{\nu}$ runs are more effective than the (5ν) run. This is shown in figures 8 and 9. In the left panel of figure 8, there is a very small sliver of allowed $\sin^2\theta_{23}$ in the wrong octant for true δ_{CP} in the range $[130°, 160°]$. But, the $\Delta\chi^2$ for this sliver is very close to 4. Hence, this wrong octant region can be effectively discriminated against, leading to a determination of the octant of θ_{23} for any true value of δ_{CP}.

The above set of figures also give the precision on $\sin^2\theta_{23}$ that one can obtain. This precision is the result of the precise measurement of $\sin^2 2\theta_{23}$ from the disappearance channel. From figures 4 and 5, we get $\delta(\sin^2\theta_{23}) = 0.015$ if LO is the true octant. From figures 6 and 7, we see that a 5 year ν run of T2K combined with NOνA gives $\delta(\sin^2\theta_{23}) = 0.02$ if HO is the true octant. When the T2K run is changed to $(2.5\nu + 2.5\bar{\nu})$, the precision in $\sin^2\theta_{23}$ becomes slightly worse because of the loss of statistics caused by $\bar{\nu}$ run as seen in figures 8 and 9.
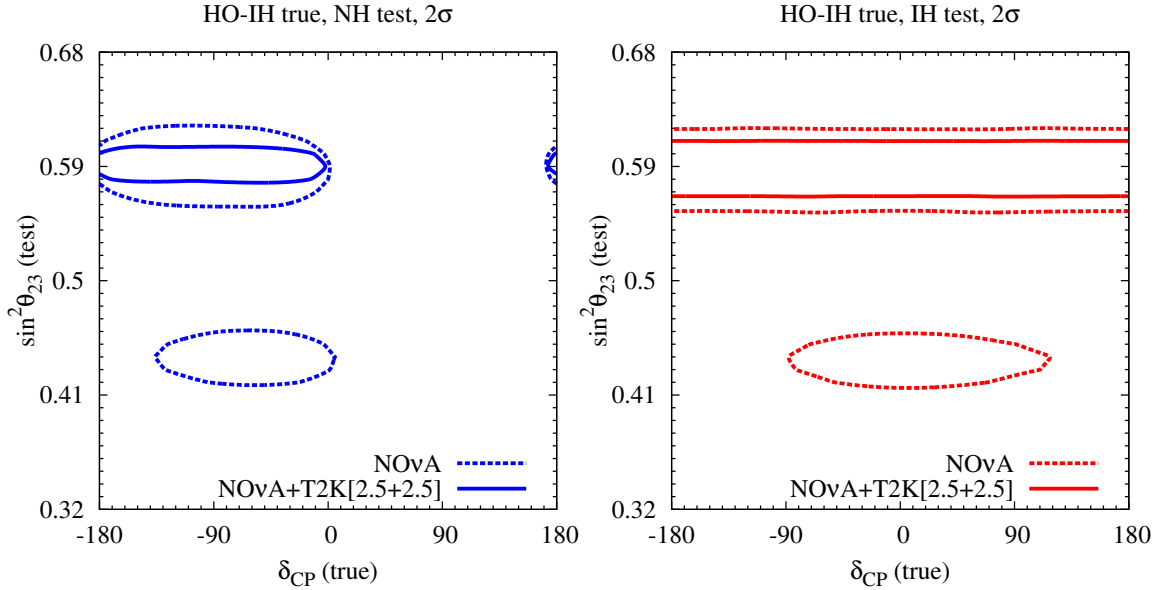

Figure 9: Allowed values of test $\sin^2\theta_{23}$ at 2σ (1 d.o.f.) C.L. as a function of true δ_{CP}. HO-IH is assumed to be the true octant-hierarchy combination. The left (right) panel corresponds to NH (IH) being the test hierarchy. Note that for T2K, equal ν and $\bar{\nu}$ runs of 2.5 years each has been assumed.

---

[4]In GLoBES, the background events for T2K are given for a 5 year ν run taken from [73]. We have taken care to do appropriate scaling of these events in computing for $(2.5\nu + 2.5\bar{\nu})$ runs.

5.2 $\Delta\chi^2$ .vs. true δ_{CP} plots

In this section, we study the behavior of $\Delta\chi^2$ between the true and the wrong octants as a function of true δ_{CP}. Here, the $\Delta\chi^2$ is computed in the following way. First, we fix the true value of δ_{CP}. We take $\sin^2\theta_{23}$ to be its best-fit value in the true octant: 0.41 for LO and 0.59 for HO. If the LO (HO) is the true octant, the test values of $\sin^2\theta_{23}$ in the HO (LO) are varied within the range $[0.5, 0.63]$ $([0.36, 0.5])$, where 0.63 (0.36) is the 2σ upper (lower) limit of the allowed range of $\sin^2\theta_{23}$. The $\Delta\chi^2$ is computed between the spectra with the best-fit $\sin^2\theta_{23}$ of the true octant and that with various test values in the wrong octant and is marginalized over other neutrino parameters, especially the hierarchy, $\sin^2 2\theta_{13}$ and δ_{CP}. Figures 10 and 11 show the minimum of this $\Delta\chi^2$ .vs. the true value of δ_{CP}.

From figure 10, we see that the NOνA data by itself can almost rule out the wrong octant at 2σ, if LO is the true octant. We see that the $\Delta\chi^2$ dips just below 4 for true $\delta_{\mathrm{CP}} \sim 0(180°)$ if the true hierarchy is NH (IH). But, as argued earlier, this small allowed region can be effectively discriminated because of the relatively large $\Delta\chi^2$. If HO is the true octant, then NOνA data is not sufficient to rule out the wrong octant as seen in figure 11. In fact, the wrong octant can be ruled out only for about half of the true δ_{CP} values. As illustrated in figures 10 and 11, addition of T2K data improves the octant determination ability significantly.
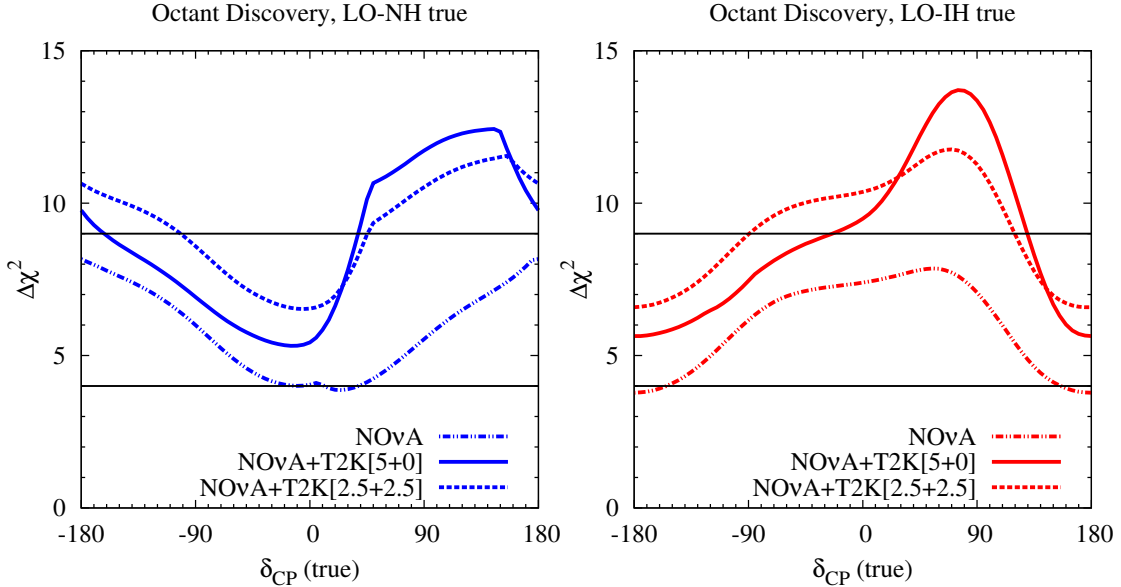

Figure 10: Octant resolving capability as a function of true δ_{CP} for various set-ups . In these plots, LO is assumed to be the true octant. The left (right) panel corresponds to NH (IH) being the true hierarchy.
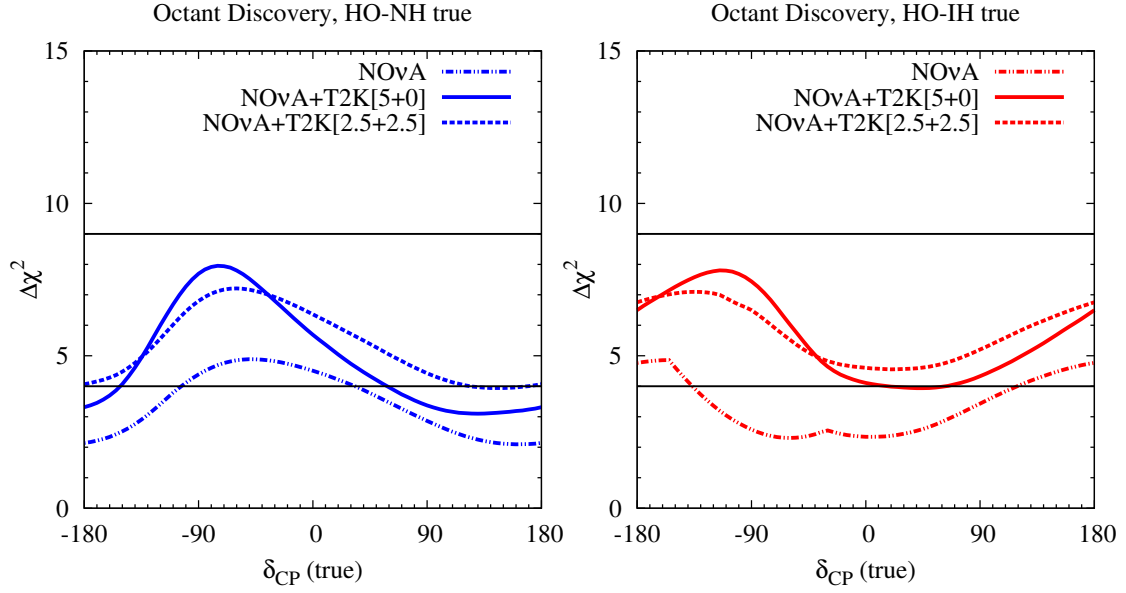
Figure 11: Octant resolving capability as a function of true δ_{CP} for various set-ups . In these plots, HO is assumed to be the true octant. The left (right) panel corresponds to NH (IH) being the true hierarchy.

From figure 10, we see that the combined data from NOνA and T2K (5ν) give a 2σ octant discrimination for all values of true δ_{CP} if LO is the true octant. From figure 11, we see that this combined data can rule out the wrong octant at 2σ for HO-IH, but not for HO-NH. The problem of HO-NH can be solved if the T2K has equal ν and $\bar{\nu}$ runs of 2.5 years each. This change improves the octant determination for the unfavorable values of true δ_{CP} (where $\Delta\chi^2$ is minimum) for all four combinations of hierarchy and octant. In particular, for the case of HO-NH, it leads to a complete ruling out of the wrong octant at 2σ for all values of true δ_{CP}. Thus, balanced runs of T2K in $\nu - \bar{\nu}$ mode is preferred over a pure ν run because of better octant determination capability.

Figures 10 and 11 show that the combined data from NOνA and T2K has a better overall octant resolving capability if LO is the true octant. We found out that this feature of LO being more favorable compared to HO is a consequence of marginalization over the oscillation parameters (mainly δ_{CP}) and the systematic uncertainties. We checked that in the absence of any kind of marginalization $\Delta\chi^2_{\mathrm{HO}}$ is consistently larger than $\Delta\chi^2_{\mathrm{LO}}$.

Before we summarize, we would like to address a non-trivial issue. As mentioned earlier, MINOS favors a non-maximal value of $\sin^2 2\theta_{\mathrm{eff}} = 0.94$. θ_{23} values calculated from this $\sin^2 2\theta_{\mathrm{eff}}$ value will not be complimentary and both LO and HO values will be closer to $45°$, compared to what we have in [13]. Octant resolving capability with these inputs for θ_{23} will be more challenging. This issue is under study [77].

6 Summary and Conclusions

Recently, the preliminary results from MINOS experiment have indicated that θ_{23} is not maximal. This raises the question of the true octant of θ_{23} *i.e.* whether $\theta_{23} < \pi/4$ (LO) or $\theta_{23} > \pi/4$ (HO). ν_e appearance searches at the presently running T2K and upcoming NOνA experiments are sensitive to the octant, especially in light of moderately large θ_{13}. The main difficulty in θ_{23}-octant resolution stems from octant-$\delta_{\rm CP}$ degeneracy. We explored this degeneracy in detail and found that balanced neutrino and anti-neutrino exposures are mandatory to overcome this problem. This is because the octant-$\delta_{\rm CP}$ combinations, which have degenerate probabilities in the neutrino data are free of this degeneracy in the anti-neutrino data and vice-verse. We also studied the prospects of T2K and NOνA to improve the precision in θ_{23}. The ν_μ disappearance data leads to two degenerate solutions of $\sin^2\theta_{23}$, one in each octant. If LO (HO) is the true octant, the expected precision will be $\delta(\sin^2\theta_{23}) = 0.015$ (0.02). The ν_e appearance data can resolve the octant degeneracy. NOνA alone can rule out the wrong octant at 2σ if LO is true, independently of hierarchy and $\delta_{\rm CP}$. Combined data from T2K and NOνA can establish the correct octant at 2σ for any combination of hierarchy, octant and $\delta_{\rm CP}$ provided T2K has equal 2.5 years of exposure in both neutrino and anti-neutrino modes rather than a full 5 years neutrino run.

A Events .vs. $\delta_{\rm CP}$

In this appendix, we consider the variation of appearance events as a function of $\delta_{\rm CP}$ in both ν and $\bar{\nu}$ modes.
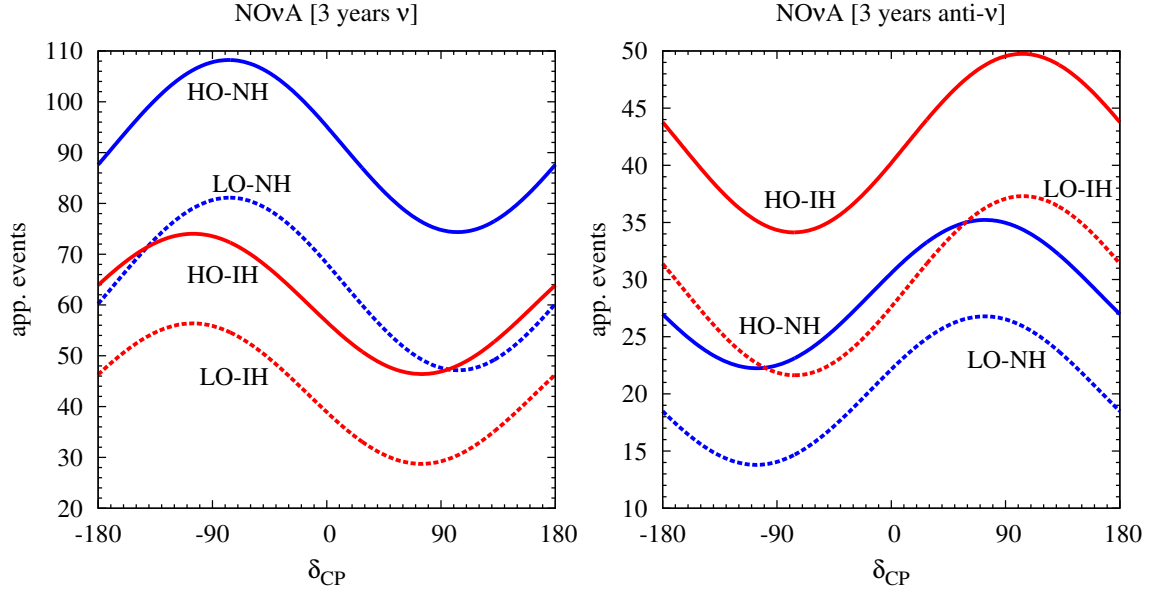
Figure 12: Total appearance events rates for all possible combinations of octant and hierarchy as a function of the δ_{CP}. The left (right) panel is for ν ($\bar{\nu}$) running. These plots are for NOνA (L=810 km), $\sin^2 2\theta_{13} = 0.089$. For LO(HO), $\sin^2 \theta_{23} = 0.41(0.59)$.
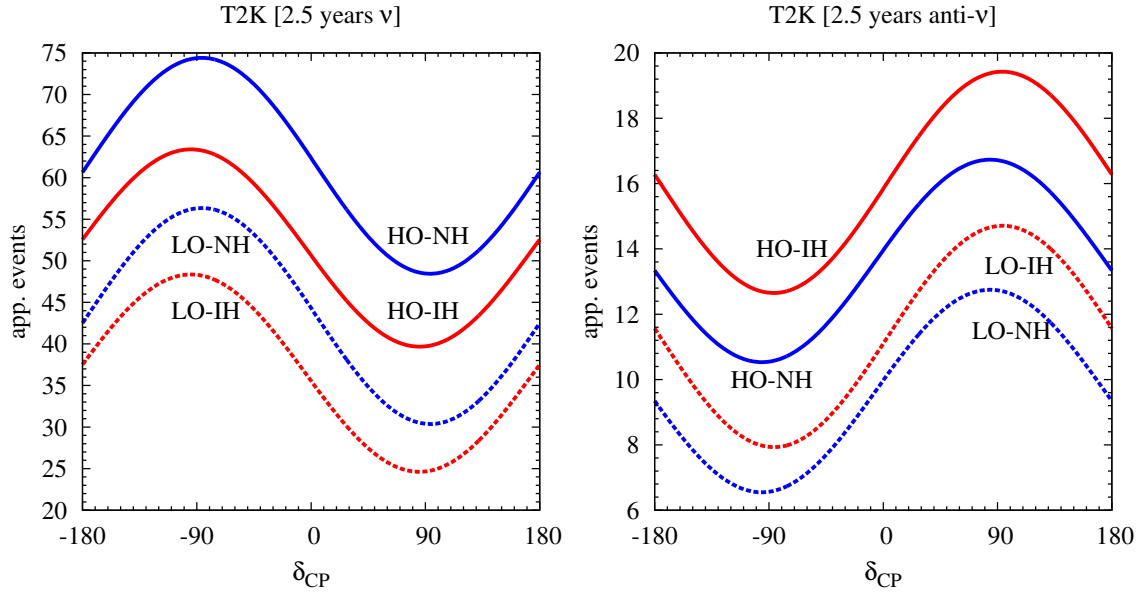

Figure 13: Total appearance events rates for all possible combinations of octant and hierarchy as a function of the δ_{CP}. The left (right) panel is for ν ($\bar{\nu}$) running. These plots are for T2K (L=295 km), $\sin^2 2\theta_{13} = 0.089$. For LO(HO), $\sin^2 \theta_{23} = 0.41(0.59)$.

In figure 12, we show the variation of $\nu_\mu \to \nu_e$ appearance events .vs. δ_{CP} for NOνA in

both ν and $\bar{\nu}$ modes. We see from the left panel (ν events) that the combinations HO-NH and LO-IH are well separated but the other two combinations- HO-IH and LO-NH have essentially the same event numbers. But in the right panel ($\bar{\nu}$ events), HO-IH and LO-NH are well separated and the other two combinations are nearly degenerate. Thus, we see that the unfavorable combinations in ν mode are favorable in $\bar{\nu}$ mode and vice-verse. This feature is seen in the event rates for T2K also as shown in figure 13 where we have assumed T2K to have 2.5 years of each neutrino and anti-neutrino run .

B   Allowed regions in test $\delta_{\rm CP}$ - test $\sin^2 \theta_{23}$ plane

In section 3, we saw that the CP conserving values of $\delta_{\rm CP}$ pose the biggest challenge in octant determination. Therefore, in this appendix, we simulate T2K and NOνA data for true $\delta_{\rm CP} = 0$ and analyze it. Figures 14-17 are drawn for each of the four possible combinations of true hierarchy and true octant. These figures show the regions allowed by the data in the test $\delta_{\rm CP}$ - test $\sin^2 \theta_{23}$ plane at 2σ ($\Delta\chi^2 \le 6.18$ for 2 d.o.f.).
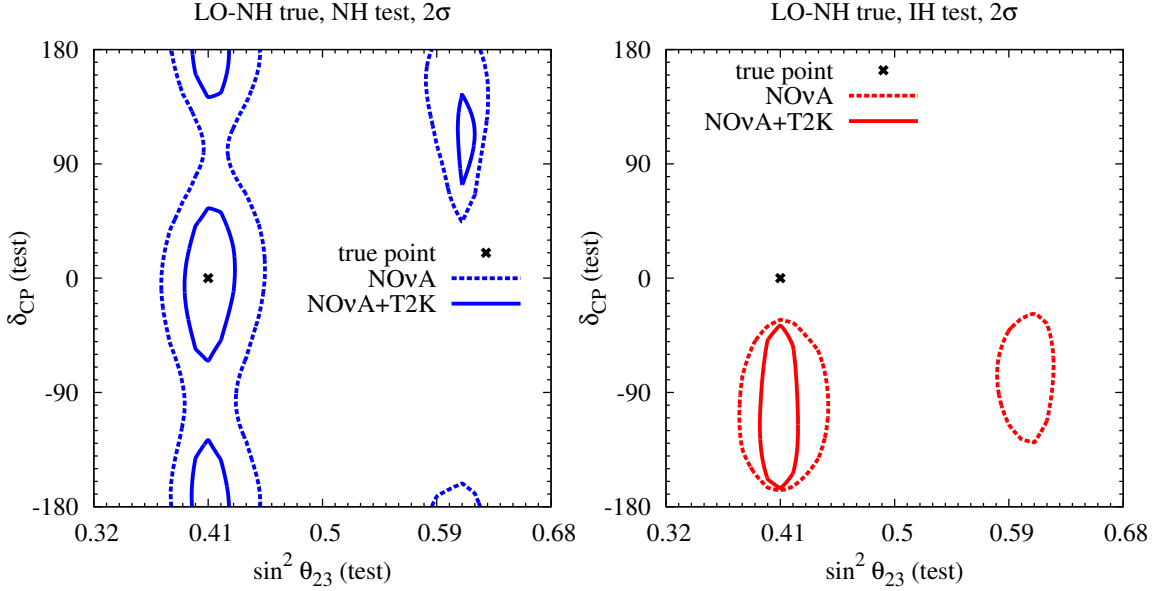

Figure 14: Allowed regions in test $\delta_{\rm CP}$ - test $\sin^2\theta_{23}$ plane at 2σ (2 d.o.f.) C.L. for true $\delta_{\rm CP} = 0$. LO-NH is assumed to be the true combination. The left (right) panel corresponds to NH (IH) being the test hierarchy.

Figure 15: Allowed regions in test δ_{CP} - test $\sin^2\theta_{23}$ plane at 2σ (2 d.o.f.) C.L. for true $\delta_{CP} = 0$. LO-IH is assumed to be the true combination. The left (right) panel corresponds to NH (IH) being the test hierarchy.
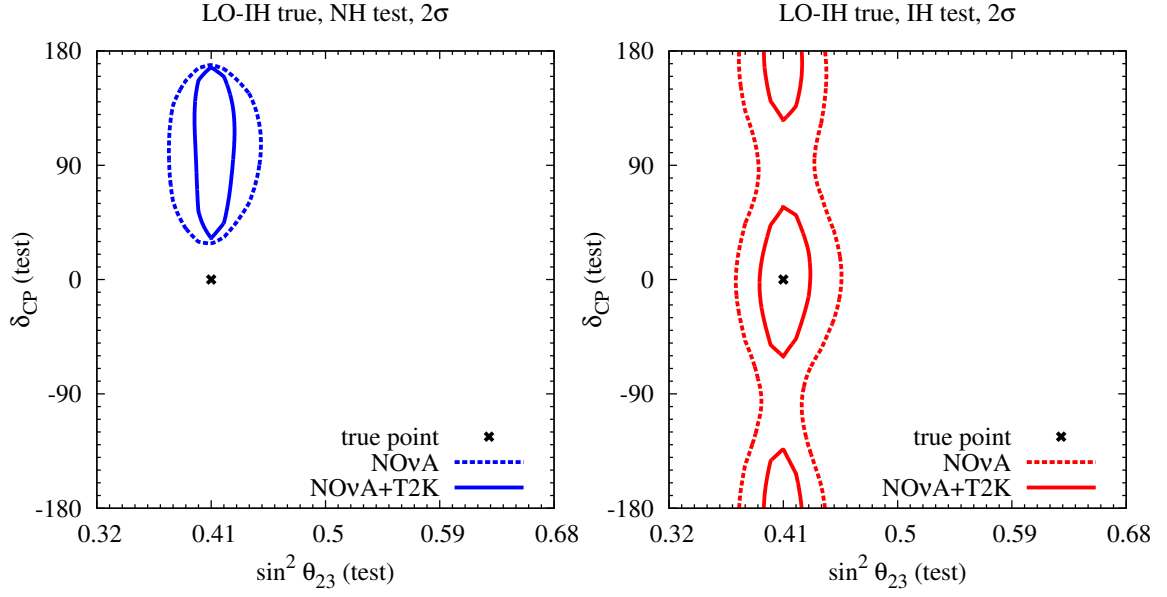

Figure 16: Allowed regions in test δ_{CP} - test $\sin^2\theta_{23}$ plane at 2σ (2 d.o.f.) C.L. for true $\delta_{CP} = 0$. HO-NH is assumed to be the true combination. The left (right) panel corresponds to NH (IH) being the test hierarchy.

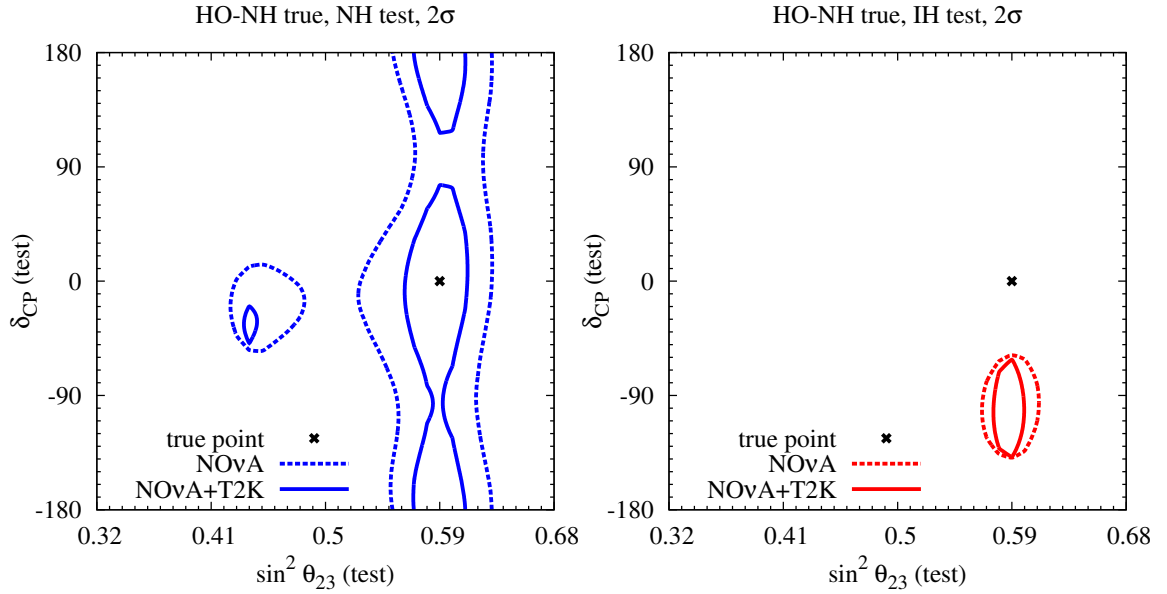**Figure 17**: Allowed regions in test δ_{CP} - test $\sin^2 \theta_{23}$ plane at 2σ (2 d.o.f.) C.L. for true $\delta_{CP} = 0$. HO-IH is assumed to be the true combination. The left (right) panel corresponds to NH (IH) being the test hierarchy.
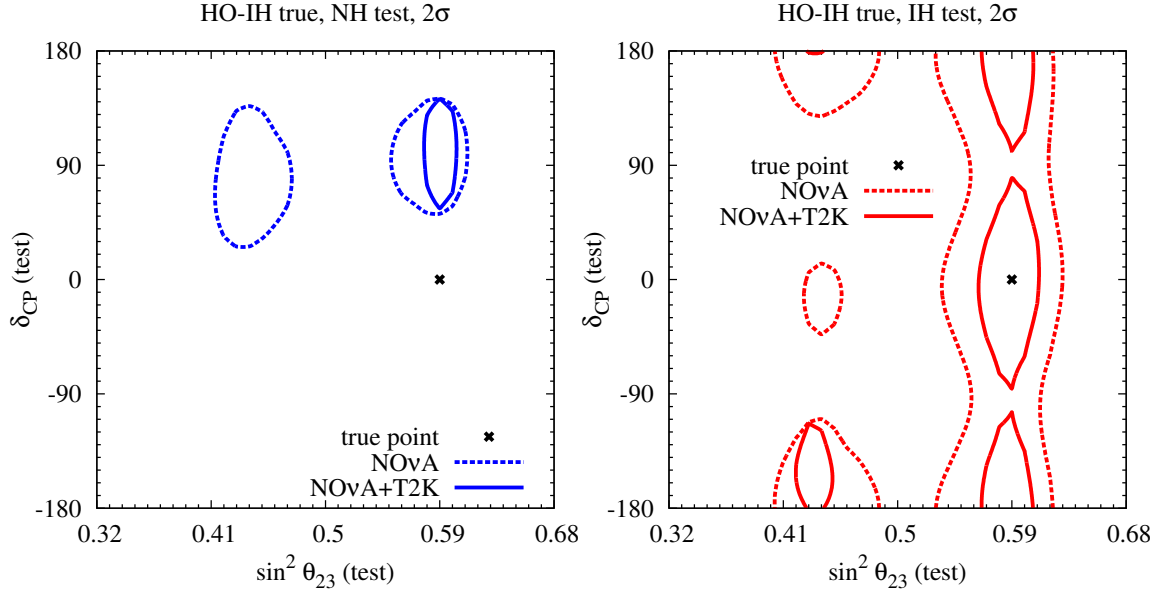
These figures illustrate that, in general, the combined data of T2K and NOνA discriminate against the wrong octant of θ_{23}. Also, note that, these figures give us the allowed ranges in both $\sin^2 \theta_{23}$ and δ_{CP} (2 d.o.f.) around the right and wrong octant for the single value of true $\delta_{CP} = 0$.

References

[1] **DAYA-BAY** Collaboration, F. An et al., *Observation of electron-antineutrino disappearance at Daya Bay*, *Phys.Rev.Lett.* **108** (2012) 171803, [arXiv:1203.1669].

[2] **RENO** Collaboration, J. Ahn et al., *Observation of Reactor Electron Antineutrino Disappearance in the RENO Experiment*, *Phys.Rev.Lett.* **108** (2012) 191802, [arXiv:1204.0626].

[3] **DAYA-BAY** Collaboration, D. Dwyer, *Improved measurement of electron–5antineutrino disappearance at daya bay*, 2012. Talk given at the Neutrino 2012 Conference, June 3-9, 2012, Kyoto, Japan, http://neu2012.kek.jp/.

[4] **RENO** Collaboration, S. Kim, *Observation of reactor antineutrino disappearance at reno*, 2012. Talk given at the Neutrino 2012 Conference, June 3-9, 2012, Kyoto, Japan, http://neu2012.kek.jp/.

[5] **T2K** Collaboration, K. Abe et al., *Indication of Electron Neutrino Appearance from an Accelerator-produced Off-axis Muon Neutrino Beam*, *Phys.Rev.Lett.* **107** (2011) 041801, [arXiv:1106.2822].

[6] **T2K** Collaboration, T. Nakaya, *New results from t2k*, 2012. Talk given at the Neutrino 2012 Conference, June 3-9, 2012, Kyoto, Japan, http://neu2012.kek.jp/.

[7] **MINOS** Collaboration, P. Adamson et al., *Improved search for muon-neutrino to electron-neutrino oscillations in MINOS*, *Phys.Rev.Lett.* **107** (2011) 181802, [arXiv:1108.0015].

[8] **MINOS** Collaboration, R. Nichol, *Final MINOS Results*, 2012. Talk given at the Neutrino 2012 Conference, June 3-9, 2012, Kyoto, Japan, http://neu2012.kek.jp/.

[9] **Double Chooz** Collaboration, Y. Abe et al., *Indication for the disappearance of reactor electron antineutrinos in the Double Chooz experiment*, *Phys.Rev.Lett.* **108** (2012) 131801, [arXiv:1112.6353].

[10] **Double Chooz** Collaboration, Y. Abe et al., *Reactor electron antineutrino disappearance in the Double Chooz experiment*, arXiv:1207.6632.

[11] D. Forero, M. Tortola, and J. Valle, *Global status of neutrino oscillation parameters after Neutrino-2012*, *Phys.Rev.* **D86** (2012) 073012, [arXiv:1205.4018].

[12] G. Fogli, E. Lisi, A. Marrone, D. Montanino, A. Palazzo, et al., *Global analysis of neutrino masses, mixings and phases: entering the era of leptonic CP violation searches*, *Phys.Rev.* **D86** (2012) 013012, [arXiv:1205.5254].

[13] M. Gonzalez-Garcia, M. Maltoni, J. Salvado, and T. Schwetz, *Global fit to three neutrino mixing: critical look at present precision*, arXiv:1209.3023.

[14] J. Hewett, H. Weerts, R. Brock, J. Butler, B. Casey, et al., *Fundamental Physics at the Intensity Frontier*, arXiv:1205.2671.

[15] H. Minakata, *Phenomenology of future neutrino experiments with large theta(13)*, 2012. Talk given at the Neutrino 2012 Conference, June 3-9, 2012, Kyoto, Japan, http://neu2012.kek.jp/.

[16] Y. Itow, *Atmospheric neutrinos: Results from running experiments*, 2012. Talk given at the Neutrino 2012 Conference, June 3-9, 2012, Kyoto, Japan, http://neu2012.kek.jp/.

[17] R. Mohapatra and A. Smirnov, *Neutrino Mass and New Physics*, *Ann.Rev.Nucl.Part.Sci.* **56** (2006) 569–628, [hep-ph/0603118].

[18] C. H. Albright and M.-C. Chen, *Model Predictions for Neutrino Oscillation Parameters*, *Phys.Rev.* **D74** (2006) 113006, [hep-ph/0608137].

[19] C. H. Albright, A. Dueck, and W. Rodejohann, *Possible Alternatives to Tri-bimaximal Mixing*, *Eur.Phys.J.* **C70** (2010) 1099–1110, [arXiv:1004.2798].

[20] S. F. King and C. Luhn, *Neutrino Mass and Mixing with Discrete Symmetry*, arXiv:1301.1340.

[21] T. Fukuyama and H. Nishiura, *Mass matrix of Majorana neutrinos*, hep-ph/9702253.

[22] R. N. Mohapatra and S. Nussinov, *Bimaximal neutrino mixing and neutrino mass matrix*, *Phys.Rev.* **D60** (1999) 013002, [hep-ph/9809415].

[23] C. Lam, *A 2-3 symmetry in neutrino oscillations*, *Phys.Lett.* **B507** (2001) 214–218, [hep-ph/0104116].

[24] P. Harrison and W. Scott, *mu - tau reflection symmetry in lepton mixing and neutrino oscillations*, *Phys.Lett.* **B547** (2002) 219–228, [hep-ph/0210197].

[25] T. Kitabayashi and M. Yasue, *S(2L) permutation symmetry for left-handed mu and tau families and neutrino oscillations in an SU(3)-L x SU(1)-N gauge model*, *Phys.Rev.* **D67** (2003) 015006, [hep-ph/0209294].

[26] W. Grimus and L. Lavoura, *A Discrete symmetry group for maximal atmospheric neutrino mixing*, *Phys.Lett.* **B572** (2003) 189–195, [[hep-ph/0305046](hep-ph/0305046)].

[27] A. Ghosal, *An SU(2)(L) x U(1)(Y) model with reflection symmetry in view of recent neutrino experimental result*, [hep-ph/0304090](hep-ph/0304090).

[28] Y. Koide, *Universal texture of quark and lepton mass matrices with an extended flavor 2-¿3 symmetry*, *Phys.Rev.* **D69** (2004) 093001, [[hep-ph/0312207](hep-ph/0312207)].

[29] R. Mohapatra and W. Rodejohann, *Broken mu-tau symmetry and leptonic CP violation*, *Phys.Rev.* **D72** (2005) 053001, [[hep-ph/0507312](hep-ph/0507312)].

[30] E. Ma, *Plato's fire and the neutrino mass matrix*, *Mod.Phys.Lett.* **A17** (2002) 2361–2370, [[hep-ph/0211393](hep-ph/0211393)].

[31] E. Ma and G. Rajasekaran, *Softly broken A(4) symmetry for nearly degenerate neutrino masses*, *Phys.Rev.* **D64** (2001) 113012, [[hep-ph/0106291](hep-ph/0106291)].

[32] K. Babu, E. Ma, and J. Valle, *Underlying A(4) symmetry for the neutrino mass matrix and the quark mixing matrix*, *Phys.Lett.* **B552** (2003) 207–213, [[hep-ph/0206292](hep-ph/0206292)].

[33] W. Grimus and L. Lavoura, *S(3) x Z(2) model for neutrino mass matrices*, *JHEP* **0508** (2005) 013, [[hep-ph/0504153](hep-ph/0504153)].

[34] E. Ma, *Tetrahedral family symmetry and the neutrino mixing matrix*, *Mod.Phys.Lett.* **A20** (2005) 2601–2606, [[hep-ph/0508099](hep-ph/0508099)].

[35] M. Raidal, *Relation between the neutrino and quark mixing angles and grand unification*, *Phys.Rev.Lett.* **93** (2004) 161801, [[hep-ph/0404046](hep-ph/0404046)].

[36] H. Minakata and A. Y. Smirnov, *Neutrino mixing and quark-lepton complementarity*, *Phys.Rev.* **D70** (2004) 073009, [[hep-ph/0405088](hep-ph/0405088)].

[37] J. Ferrandis and S. Pakvasa, *Quark-lepton complenmentarity relation and neutrino mass hierarchy*, *Phys.Rev.* **D71** (2005) 033004, [[hep-ph/0412038](hep-ph/0412038)].

[38] S. Antusch, S. F. King, and R. N. Mohapatra, *Quark-lepton complementarity in unified theories*, *Phys.Lett.* **B618** (2005) 150–161, [[hep-ph/0504007](hep-ph/0504007)].

[39] G. L. Fogli and E. Lisi, *Tests of three flavor mixing in long baseline neutrino oscillation experiments*, *Phys.Rev.* **D54** (1996) 3667–3670, [[hep-ph/9604415](hep-ph/9604415)].

[40] V. Barger, D. Marfatia, and K. Whisnant, *Breaking eight fold degeneracies in neutrino CP violation, mixing, and mass hierarchy*, *Phys.Rev.* **D65** (2002) 073023, [[hep-ph/0112119](hep-ph/0112119)].

[41] H. Minakata, H. Nunokawa, and S. J. Parke, *Parameter degeneracies in neutrino oscillation measurement of leptonic CP and T violation*, *Phys.Rev.* **D66** (2002) 093012, [[hep-ph/0208163](hep-ph/0208163)].

[42] J. Burguet-Castell, M. Gavela, J. Gomez-Cadenas, P. Hernandez, and O. Mena, *On the Measurement of leptonic CP violation*, *Nucl.Phys.* **B608** (2001) 301–318, [[hep-ph/0103258](hep-ph/0103258)].

[43] H. Minakata and H. Nunokawa, *Exploring neutrino mixing with low-energy superbeams*, *JHEP* **0110** (2001) 001, [[hep-ph/0108085](hep-ph/0108085)].

[44] H. Minakata, H. Sugiyama, O. Yasuda, K. Inoue, and F. Suekane, *Reactor measurement of theta(13) and its complementarity to long baseline experiments*, *Phys.Rev.* **D68** (2003) 033017, [[hep-ph/0211111](hep-ph/0211111)].

[45] K. Hiraide, H. Minakata, T. Nakaya, H. Nunokawa, H. Sugiyama, et al., *Resolving theta(23) degeneracy by accelerator and reactor neutrino oscillation experiments*, *Phys.Rev.* **D73** (2006) 093008, [`hep-ph/0601258`].

[46] A. Donini, D. Meloni, and P. Migliozzi, *The Silver channel at the neutrino factory*, *Nucl.Phys.* **B646** (2002) 321–349, [`hep-ph/0206034`].

[47] D. Meloni, *Solving the octant degeneracy with the Silver channel*, *Phys.Lett.* **B664** (2008) 279–284, [`arXiv:0802.0086`].

[48] S. Antusch, P. Huber, J. Kersten, T. Schwetz, and W. Winter, *Is there maximal mixing in the lepton sector?*, *Phys.Rev.* **D70** (2004) 097302, [`hep-ph/0404268`].

[49] H. Minakata, M. Sonoyama, and H. Sugiyama, *Determination of theta(23) in long-baseline neutrino oscillation experiments with three-flavor mixing effects*, *Phys.Rev.* **D70** (2004) 113012, [`hep-ph/0406073`].

[50] M. Gonzalez-Garcia, M. Maltoni, and A. Y. Smirnov, *Measuring the deviation of the 2-3 lepton mixing from maximal with atmospheric neutrinos*, *Phys.Rev.* **D70** (2004) 093005, [`hep-ph/0408170`].

[51] D. Choudhury and A. Datta, *Detecting matter effects in long baseline experiments*, *JHEP* **0507** (2005) 058, [`hep-ph/0410266`].

[52] S. Choubey and P. Roy, *Probing the deviation from maximal mixing of atmospheric neutrinos*, *Phys.Rev.* **D73** (2006) 013006, [`hep-ph/0509197`].

[53] D. Indumathi, M. Murthy, G. Rajasekaran, and N. Sinha, *Neutrino oscillation probabilities: Sensitivity to parameters*, *Phys.Rev.* **D74** (2006) 053004, [`hep-ph/0603264`].

[54] T. Kajita, H. Minakata, S. Nakayama, and H. Nunokawa, *Resolving eight-fold neutrino parameter degeneracy by two identical detectors with different baselines*, *Phys.Rev.* **D75** (2007) 013006, [`hep-ph/0609286`].

[55] K. Hagiwara and N. Okamura, *Solving the degeneracy of the lepton-flavor mixing angle theta(ATM) by the T2KK two detector neutrino oscillation experiment*, *JHEP* **0801** (2008) 022, [`hep-ph/0611058`].

[56] A. Samanta and A. Y. Smirnov, *The 2-3 mixing and mass split: atmospheric neutrinos and magnetized spectrometers*, *JHEP* **1107** (2011) 048, [`arXiv:1012.0360`].

[57] **T2K** Collaboration, Y. Itow et al., *The JHF-Kamioka neutrino project*, `hep-ex/0106019`.

[58] **NOvA** Collaboration, D. Ayres et al., *NOvA: Proposal to build a 30 kiloton off-axis detector to study nu(mu) to nu(e) oscillations in the NuMI beamline*, `hep-ex/0503053`.

[59] **NOνA** Collaboration, R. Patterson, *The NOνA Experiment: Status and Outlook*, 2012. Talk given at the Neutrino 2012 Conference, June 3-9, 2012, Kyoto, Japan, `http://neu2012.kek.jp/`.

[60] H. Nunokawa, S. J. Parke, and R. Zukanovich Funchal, *Another possible way to determine the neutrino mass hierarchy*, *Phys.Rev.* **D72** (2005) 013009, [`hep-ph/0503283`].

[61] A. de Gouvea, J. Jenkins, and B. Kayser, *Neutrino mass hierarchy, vacuum oscillations, and vanishing —U(e3)—*, *Phys.Rev.* **D71** (2005) 113009, [`hep-ph/0503079`].

[62] S. K. Raut, *Effect of non-zero theta(13) on the measurement of theta(23)*, `arXiv:1209.5658`.

[63] **Particle Data Group** Collaboration, J. Beringer et al., *Review of Particle Physics (RPP)*, *Phys.Rev.* **D86** (2012) 010001.

[64] E. K. Akhmedov, R. Johansson, M. Lindner, T. Ohlsson, and T. Schwetz, *Series expansions for three flavor neutrino oscillation probabilities in matter*, *JHEP* **0404** (2004) 078, [hep-ph/0402175].

[65] A. Cervera, A. Donini, M. Gavela, J. Gomez Cadenas, P. Hernandez, et al., *Golden measurements at a neutrino factory*, *Nucl.Phys.* **B579** (2000) 17–55, [hep-ph/0002108].

[66] M. Freund, *Analytic approximations for three neutrino oscillation parameters and probabilities in matter*, *Phys.Rev.* **D64** (2001) 053003, [hep-ph/0103300].

[67] L. Wolfenstein, *Neutrino oscillations in matter*, *Phys. Rev.* **D17** (1978) 2369–2374.

[68] O. Mena and S. J. Parke, *Untangling CP violation and the mass hierarchy in long baseline experiments*, *Phys.Rev.* **D70** (2004) 093011, [hep-ph/0408070].

[69] S. Prakash, S. K. Raut, and S. U. Sankar, *Getting the Best Out of T2K and NOvA*, *Phys.Rev.* **D86** (2012) 033012, [arXiv:1201.6485].

[70] P. Huber, M. Lindner, and W. Winter, *Simulation of long-baseline neutrino oscillation experiments with GLoBES (General Long Baseline Experiment Simulator)*, *Comput.Phys.Commun.* **167** (2005) 195, [hep-ph/0407333].

[71] P. Huber, J. Kopp, M. Lindner, M. Rolinec, and W. Winter, *New features in the simulation of neutrino oscillation experiments with GLoBES 3.0: General Long Baseline Experiment Simulator*, *Comput.Phys.Commun.* **177** (2007) 432–438, [hep-ph/0701187].

[72] P. Huber, M. Lindner, T. Schwetz, and W. Winter, *First hint for CP violation in neutrino oscillations from upcoming superbeam and reactor experiments*, *JHEP* **0911** (2009) 044, [arXiv:0907.1896].

[73] M. Fechner, *Détermination des performances attendues sur la recherche de l'oscillation numu to nue dans l'expérience T2K depuis l'étude des données recueillies dans l'expérience K2K*, . Presented on 9 May 2006.

[74] **NOνA** Collaboration, D. Ayres et al., *The NOνA Technical Design Report*, tech. rep., 2007. FERMILAB-DESIGN-2007-01.

[75] S. K. Agarwalla, S. Prakash, S. K. Raut, and S. U. Sankar, *Potential of optimized NOvA for large θ_{13} & combined performance with a LArTPC & T2K*, *JHEP* **1212** (2012) 075, [arXiv:1208.3644].

[76] **Daya Bay** Collaboration, X. Qian, *Improved Measurement of Electron-antineutrino Disappearance at Daya Bay*, 2012. Talk given at the NuFact 2012 Conference, July 23-28, 2012, Williamsburg, USA, http://www.jlab.org/conferences/nufact12/.

[77] S. K. Agarwalla, S. Prakash, and S. U. Sankar, *work in progress*, .